amt-2020-240

Thank you for reviewing the manuscript and providing constructive comments. We have made edits to the manuscript incorporated with your suggestions. Reviewers' comments are shown in black, our response to each comment is shown in blue, and changes to the manuscript are shown in red.

Reviewer #2:
Recommendation: I only found one thing to change, in the Introduction, noted below. Otherwise this a fine original paper which is perfectly suitable for publication in AMT. My comments below are mainly for the authors as I have no minor or major revisions to ask for.

Abstract: The abstract is a clear and concise description of the paper. Fine as is.

Thank you for the comment.

1. Introduction: You write " One limitation is that a ground-based Doppler radar has to be located outside of the radial distance between the radar and the storm center in order to sample the full tangential component of the vortex circulation accurately." I think you meant to write that the radar has to be outside the radius of maximum wind.It is impossible for the radar to be located farther away than the storm center to radar distance!

Thank you for the comment. We have revised the sentence.

One limitation is that the radial distance between the radar and the storm center has to be large enough to sample the tangential component of the vortex circulation in order to minimize the geometric distortion.

2. Data Sets and Methodology: This section nicely summarizes the data procedures. I am curious why the SAMURAI analyses were interpolated to a polar array while the VoRTRAC were apparently still in Cartesian form. If in fact the end result of the Vortrac analyses also ended up in polar form that should be stated here.

Thank you for the comment. We have added a comment to the manuscript to clarify.

The gridded data was further analyzed using the Vortex Objective Radar Tracking and Circulation (VORTRAC) software in LROSE to interpolate onto a cylindrical coordinate and obtain the kinematic structure by the improved GVTD algorithm formulated in section 3.1.

3. The GVTD technique improvement: 3.1: a lot of math shown here but all of it necessary. I wonder if there was earlier work on data gaps and noise influence on maximum wavenumber to retrieve. Probably not needed but I believe the code in GBVTD to select max wavenumber was developed originally by the late Tom Matejka for the Extended VAD which is an ancestor of the VTD. Well, probably too much detail for this paper anyway.

Thank you for the comment. We have added the reference of Matejka and Srivastava 1991.

To deal with missing data in observational radar data and reduce the influence of outliers [Matejka and Srivastava, 1991], the truncation of the Fourier series follows Lee et al. (2000) (Table 2), which is consistent with the restriction of maximum allowable gap size in Lorsolo and Aksoy (2012) .

3.2 GVTD-simplex center finding The description of the simplex minimization algorithm is a bit sparse. Maybe you should add a direct reference. Either that or remove the references to "contraction or expansion of the simplex" since you did not really explain what those terms mean. Also in the text when you mention comparisons of simplex-derived centers from different WSR88D radars you might list the locations: KMLB (Melbourne,FL) and KJAX (Jacksonville, FL). I think Harasti et al.(year?) had a nice description of many different of finding circulation centers.

Thank you for the comment. We have added the reference of Harasti et al. 2004 .

The simplex center is found by maximizing the mean tangential wind within an axisymmetric TC with three operations on a simplex: reflection, contraction, and expansion [Lee and Marks, 2000, Harasti et al., 2004].

Also you might mention that the "dynamic"centers are smooth because the spline fit is to only a few aircraft derived centers, One per pass, so one would not expect them to show as much variation as the G*VTD centers available every 5-6 minutes. also you have an independent wind field from SAMURAI TDR analyses.

Thank you for the comment. We have clarified the sentence.

The centers are interpolated from a few dynamic centers with a series of spline curves every two minutes, so the centers are connected into a continuous track.

Did you try simplex center finding on the pseudo-dual Doppler arrays? The Marks used the simplex to show variation of center with height in his airborne radar work and this was then later applied by Lee and Marks to the GBVTD.

Thank you for the comment. We have tried the simplex center finding on the pseudo-dual Doppler analysis, and the discrepancies between the simplex centers and dynamic centers are small. The retrieved wind fields are similar, as well as the asymmetric structure. Therefore, we decide to use the dynamic centers to be consistent with our future work discussing Hurricane Matthew's asymmetric structure observed by the ground-based radars.

4 Wind retrievals comparison between single Doppler and airborne dual Doppler analyses: This is the real meat of this paper and it is amazing that no one did this before. Maybe it had to wait for the development of GEVTD and SAMURAI before such a study could be done, but I think this part alone should be part of any class on radar meteorology from now on.

Thank you very much for the positive endorsement!

4.1 Wavenumber 0 tangential wind retrieval this section shows that GEVTD (both versions) capture well the wave 0 tangential wind by comparing with the pseudo dual Doppler analysis from the P3. This is a slick idea to generate 88d obs by projecting the TDR analysis on the 88d radials and then doing the VTD on those "data" rather than on the original 88d data. As I read this, I couldn't help thinking you could just as easily plopped some idealized vortex on Matthews position and used totally synthetic data to test the VTD algorithm performance. I am not suggesting you do this as you already have the SAMURAI analysis, just a thought that you did not need a "real" storm to do this part of the analysis.

Thank you for the comment. In response to this and another reviewer's comment, we have done an idealized experiment to show that the steady-state assumption of one straight flight leg to synthesize the data into one snapshot with the presence of rapidly evolving features could result in temporal aliasing and unrealistic asymmetric component retrievals. We have added a new subsection 4.3 and Figure 8 (Fig. 1 here) in the revised manuscript.

4.2 Asymmetric wind retrievals This is a very interesting discussion. I do wonder if the authors could say a bit more about the signature of the VRW in the reflectivity or is the VRW only visible in the wind field? It is easy to visualize in my mind the wave 1 asymmetry, but higher wave numbers make me think there should be a series of bumps in the dBZ, or is the reality that the asymmetries are more finer in scale, so requiring higher wave numbers? That is, are convective cells in the RMW giving rise to wind asymmetries that are then aliased onto wave 2? well, probably can't answer that with this dataset.

Thank you for the comment. Cha et al. 2020 shows the signature of the VRW in the reflectivity and the GVTD-retrieved tangential wind fields. The propagation speeds of asymmetric tangential wind and reflectivity signals are consistent with the linear wave theory, suggesting that the observed asymmetries are well described by VRW theory (Fig. 4 in Cha et al. 2020).
Figure 2 shows the azimuthal temporal evolution of wavenumber 1 and 2 of reflectivity and tangential wind in the inner eyewall region of Hurricane Matthew. The wavenumber 1 reflectivity is stationary from 1915 to 1945 UTC, whereas the wavenumber 2 reflectivity signals are also propagating, similar to the wavenumber 2 tangential wind signals. We have added the features description of the wavenumber 1 and 2 reflectivity signals in the manuscript, but the plot of reflectivity is not shown.

To test the hypothesis, the phases of maximum wavenumber 1 and wavenumber 2 tangential winds retrieved from the 5-minute single Doppler observations are examined in Fig. 7 for the temporal evolution during the first flight pass from 1907 to 1940 UTC. The amplitude and phase (Eqs. 18 and 19) of wavenumber 1 and 2 tangential winds are denoted in polar coordinates by the radius and azimuth, respectively. The wavenumber 1 tangential wind (Fig. 7a) generally stayed unchanged throughout the first pass with a magnitude between 8 and 12 m s^{-1} and phase to the E to NE (same as the wavenumber 1 reflectivity, not shown here). Environmental vertical wind shear derived from the Statistical Hurricane Intensity Prediction Scheme dataset (SHIPS) points to the northeast direction with a magnitude of 7 m s^{-1}, suggesting that the wavenumber 1 distribution is forced by the vertical wind shear to be consistently in the downshear-right quadrant.
The wavenumber 2 tangential wind (Fig. 7b) propagated cyclonically during the flight pass (same as the wavenumber 2 reflectivity, not shown here) with a magnitude up to 7 m s^{-1}. The propagation of the wavenumber 2 tangential wind is estimated to be 285

degrees from 1907 to 1940 UTC, which is 35 m s^{-1}, or 63% of V_{Tmax}. The propagation of the wavenumber 2 tangential wind is roughly consistent with linear VRW theory [Kuo et al., 1999, Cha et al., 2020].

I know that VORTRAC also can produce a MSLP estimate from the symmetric wind field. I wonder if the VTD analyses give mslp similar to the flight level data. If the wind fields agree so well I would think the pressure retrievals should also. Not necessary for this paper though.

Thank you for the comment. We have computed the perturbation pressure deficit using the gradient wind balance equation. The integrated perturbation pressure deficit retrievals from different methods agree well with the 'truth'. The analysis and RMS difference of the integrated perturbation pressure deficit are added to Table 4 in the manuscript.

The perturbation pressure deficit is integrated from r = 10 to 70 km using the gradient wind balance equation [Lee et al., 2000]. The integrated perturbation pressure deficit retrievals from different methods agree well with the "truth" ($\sim$ 1 mb RMS in general). Similar as the results of RMS difference of $V_T C_0$, including the storm motion terms decreases the RMS differences about 0.2 mb. The RMS difference of improved GVTD algorithm from the single Doppler retrieval has the least deviation from the "truth", suggesting that the perturbation pressure deficit derived from the single Doppler observations has high fidelity.

5 Conclusions the authors nicely summarize their work here and hint that there is more to be said about the analyses themselves. In this paper they have validated both methods of analysis and I imagine the next Cha et al. will go into more detail about the VRW's and other features of this dataset including the eyewall replacement. This methods-oriented paper is a fine introduction to that topic.

Thank you for the comment. Some additional analyses using the improved formulation can be found in Cha (2018), with continued analysis submitted to the peer-reviewed literature in the future.

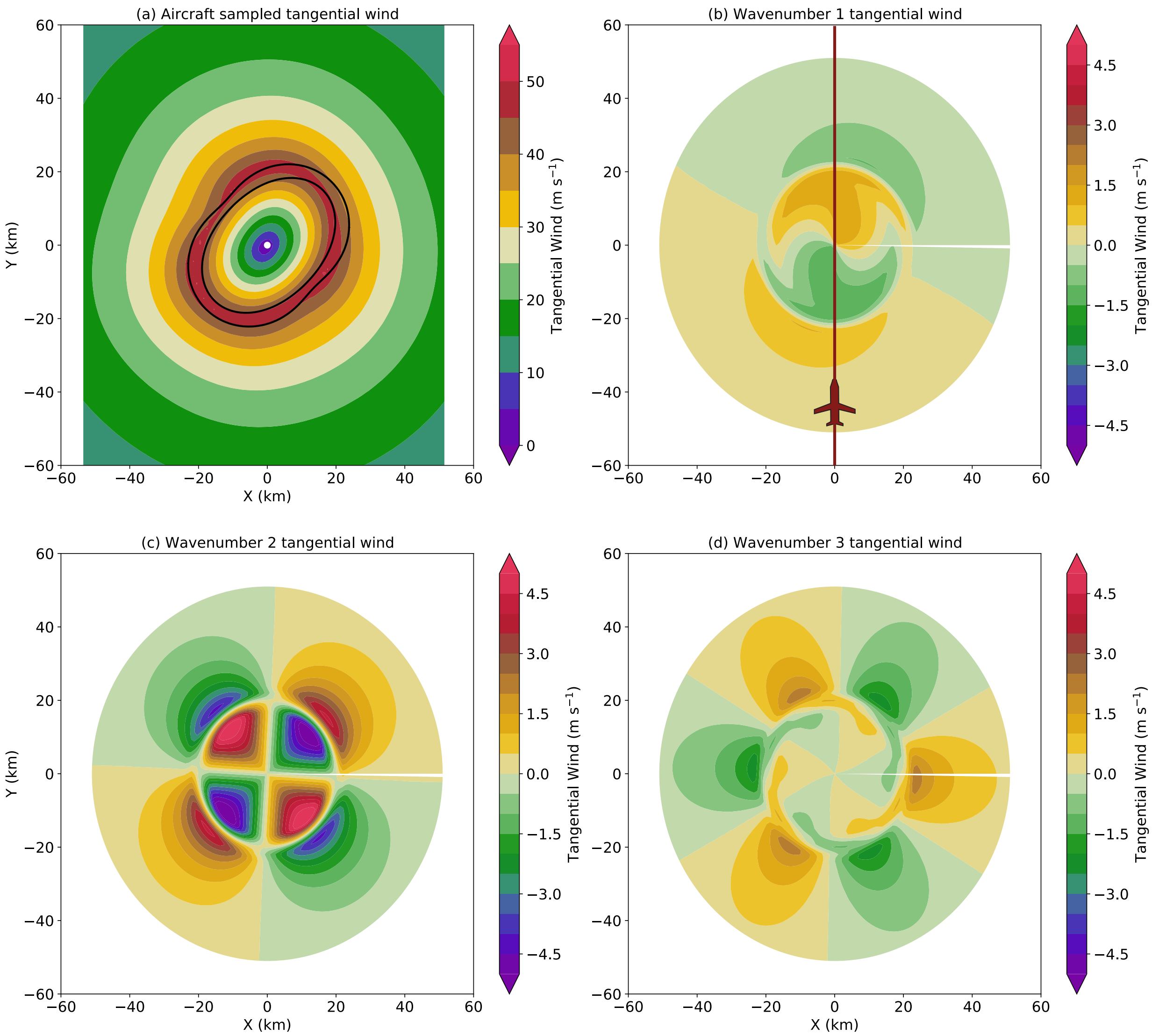

Figure 1: (a) Idealized dual-Doppler tangential wind speed retrieved from a straight flight pass through propagating wavenumber two asymmetry (color in m s^{-1}) and 50 m s^{-1} contour of time-averaged wavenumber two in black. The initial phase of the propagating wavenumber 2 tangential wind is oriented from east to west and final phase is from north to south. (b) Wavenumber 1 plus aircraft flight track from south to north, (c) Wavenumber 2, and (d) Wavenumber 3 tangential wind components retrieved by the Fourier decomposition of the tangential wind field shown in panel (a).

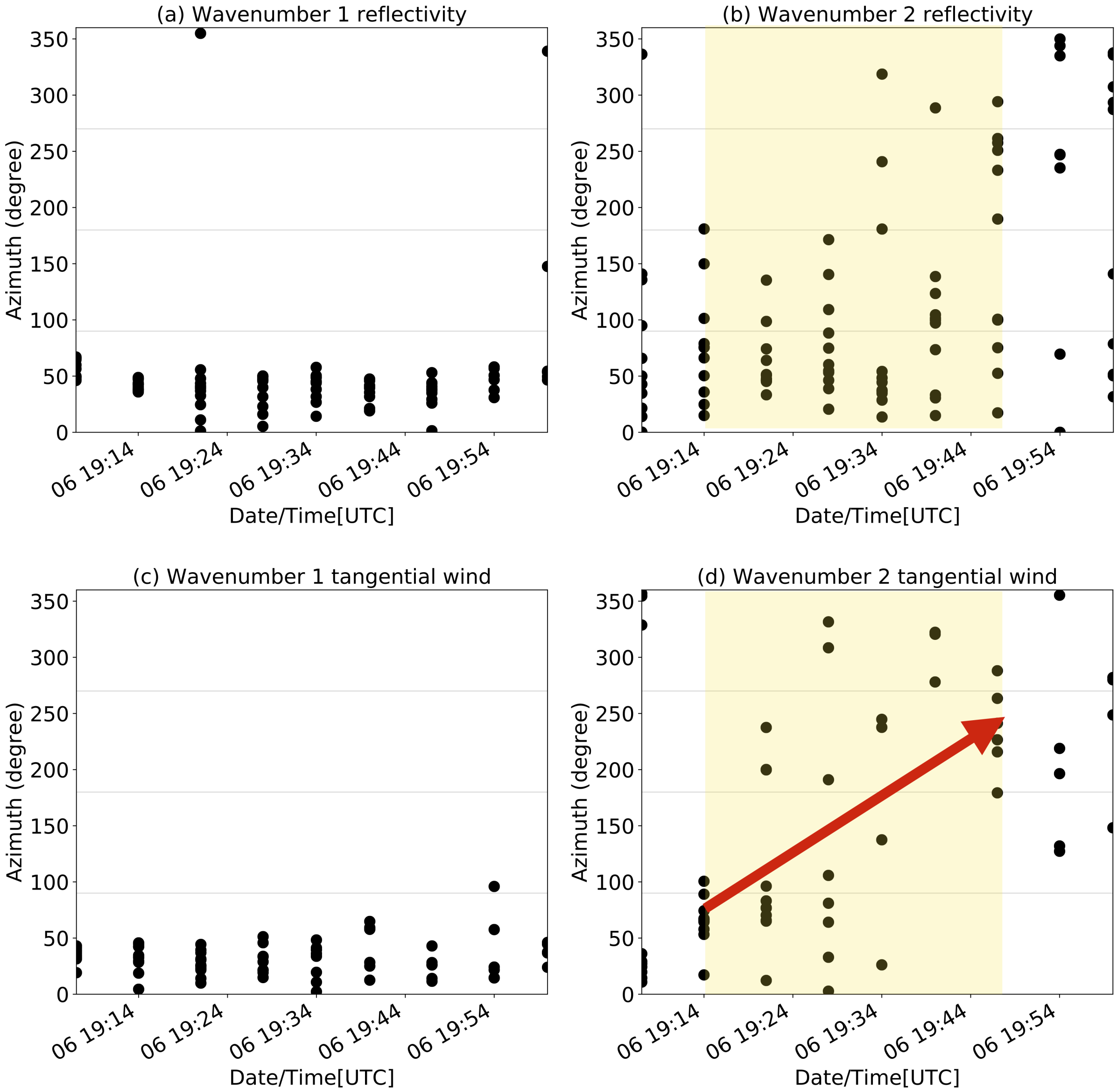

Figure 2: The azimuthal temporal evolution of wavenumber 1 and 2 of reflectivity and tangential wind in the inner eyewall region (from the radius of 15-25 km) from 1900 to 2000 UTC 6 October. The black dots are (a) Wavenumber 1 reflectivity, (b) Wavenumber 2 reflectivity, (c) Wavenumber 1 tangential wind, and (d) Wavenumber 2 tangential wind within the area from the radius of 15 to 25 km. The red arrow denotes the propagation of the median of wavenumber 2 tangential wind from 1915 to 1945 UTC, and the yellow shading illustrates the period of 1915 UTC to 1945 UTC. Adapted from Cha 2018.

References

[Cha, 2018] Cha, T.-Y. (2018). Eyewall replacement cycle of Hurricane Matthew (2016) observed by Doppler radars. *M. S. Thesis*, page Colorado State University.

[Cha et al., 2020] Cha, T.-Y., Bell, M. M., Lee, W.-C., and DesRosiers, A. J. (2020). Polygonal eyewall asymmetries during the rapid intensification of Hurricane Michael (2018). *Geophys. Res. Lett.*, 47(15):e2020GL087919.

[Harasti et al., 2004] Harasti, P. R., McAdie, C. J., Dodge, P. P., Lee, W.-C., Tuttle, J., Murillo, S. T., and Marks, F. D. (2004). Real-time implementation of Single-Doppler radar analysis methods for tropical cyclones: Algorithm improvements and use with WSR-88D display data. *Wea. Forecasting*, 19(2):219 – 239.

[Kuo et al., 1999] Kuo, H.-C., Williams, R., and Chen, J.-H. (1999). A possible mechanism for the eye rotation of Typhoon Herb. *J. Atmos. Sci.*, 56(11):1659–1673.

[Lee et al., 2000] Lee, W.-C., Jou, B. J.-D., Chang, P.-L., and Marks, F. D. (2000). Tropical cyclone kinematic structure retrieved from single-Doppler radar observations. Part III: Evolution and structures of Typhoon Alex (1987). *Mon. Wea. Rev.*, 128(12):3982–4001.

[Lee and Marks, 2000] Lee, W.-C. and Marks, F. D. (2000). Tropical cyclone kinematic structure retrieved from single-Doppler radar observations. Part II: The GBVTD-simplex center finding algorithm. *Mon. Wea. Rev.*, 128(6):1925–1936.

[Lorsolo and Aksoy, 2012] Lorsolo, S. and Aksoy, A. (2012). Wavenumber analysis of azimuthally distributed data: Assessing maximum allowable gap size. *Mon. Wea. Rev.*, 140(6):1945–1956.

[Matejka and Srivastava, 1991] Matejka, T. and Srivastava, R. C. (1991). An improved version of the Extended Velocity-Azimuth Display analysis of Single-Doppler radar data. *J. Atmos. Oceanic Technol.*, 8(4):453 – 466.